V4D:4D CONVOLUTIONAL NEURAL NETWORKS FOR VIDEO-LEVEL REPRESENTATIONS LEARNING

Anonymous authors
Paper under double-blind review

ABSTRACT

Most existing 3D CNN structures for video representation learning are clip-based methods, and do not consider video-level temporal evolution of spatio-temporal features. In this paper, we propose Video-level 4D Convolutional Neural Networks, namely V4D, to model the evolution of long-range spatio-temporal representation with 4D convolutions, as well as preserving 3D spatio-temporal representations with residual connections. We further introduce the training and inference methods for the proposed V4D. Extensive experiments are conducted on three video recognition benchmarks, where V4D achieves excellent results, surpassing recent 3D CNNs by a large margin.

1 INTRODUCTION

3D convolutional neural networks (3D CNNs) and their variants (Ji et al., 2010; Tran et al., 2015; Carreira & Zisserman, 2017; Qiu et al., 2017; Wang et al., 2018b) provide a simple extension from 2D counterparts for video representation learning. However, due to practical issues such as memory consumption and computational cost, these models are mainly used for clip-level feature learning instead of training from the whole video. In this sense, during training, the clip-based methods randomly sample a short clip (e.g., 32 frames) from the video for representation learning. During testing, they uniformly sample several clips from the whole video in a sliding window manner and calculate the prediction scores for each clip independently. Finally the prediction scores of all clips are simply averaged to yield the video-level prediction. Although achieving very competitive accuracy, these clip-based models ignore the video-level structure and long-range spatio-temporal dependency during training, as they only sample a small portion of the entire video. In fact, sometimes it could be very hard to recognize action class only with partial observation. Meanwhile, simply averaging the prediction scores of all clips could be also sub-optimal during testing. To overcome this issue, Temporal Segment Network (TSN) (Wang et al., 2016) uniformly samples multiple clips from the entire video and uses their average score to guide back-propagation during training. Thus TSN is a video-level representation learning framework. However, the inter-clip interaction and video-level fusion in TSN is only performed at very late stage, which fails to capture finer temporal structures.

In this paper, we propose a general and flexible framework for video-level representation learning, called V4D. As shown in Figure 1, to model long-range dependency in a more efficient and principled way, V4D is composed of two critical design: (1) holistic sampling strategy and (2) 4D convolutional interaction. We first introduce a video-level sampling strategy by uniformly sampling a sequence of short-term units covering the holistic video. Then we model long-range spatio-temporal dependency by designing a unique 4D residual block. Specifically, we present a 4D convolutional operation to capture inter-clip interaction, which could enhance the representation power of the original clip-level 3D CNNs. The 4D residual blocks could be easily integrated into the existing 3D CNNs to perform long-range modeling more earlier and hierarchically than TSN. We also design a specific video-level inference algorithm for V4D. Specifically, we verify the effectiveness of V4D on three video action recognition benchmarks, Mini-Kinetics (Xie et al., 2018), Kinetics-400 (Carreira & Zisserman, 2017) and Something-Something-V1 (Goyal et al., 2017). V4D structures achieve very competitive performance on these benchmarks and obtain evident performance improvement over their 3D counterparts.

2 RELATED WORKS

The architectures for video recognition can be roughly categorized into three groups: Two-stream CNNs, 3D CNNs, and long-term modeling framework .

2.1 TWO-STREAM CNNS

Two-stream architecture was first proposed by (Simonyan & Zisserman, 2014), where one stream is used for learning from RGB images, and the other one is applied for modeling optical flow. The results produced by the two streams are then fused at later stages, yielding the final prediction. Two-stream CNNs have achieved impressive results on various video recognition tasks. However, the main drawback is that the computation of optical flow often takes rather long time with expensive resource explored. Recent effort has been devoted to reducing the computational cost on modeling optical flow, such as (Dosovitskiy et al., 2015; Sun et al., 2018; Piergiovanni & Ryoo, 2018; Zhang et al., 2016). Two-stream input and fusion is a general method to boost the accuracy of various CNN structures, which is orthogonal with our proposed V4D.

2.2 3D CNNS

3D CNNs have recently been proposed (Tran et al., 2015; Carreira & Zisserman, 2017; Wang et al., 2018a;b; Feichtenhofer et al., 2018). By considering a video as a stack of frames, it is natural to utilize 3D convolutions directly on video data. However, 3D CNNs often have a larger number of model parameters, which require more training data to achieve high performance. Recent experimental results on large scale benchmark of Kinetics-400 (Carreira & Zisserman, 2017), as reported in (Wang et al., 2018b; Feichtenhofer et al., 2018), show that 3D CNNs can surpass their 2D counterparts in most cases, even on par with or better than the two-stream 2D CNNs. It is noteworthy that most of 3D CNNs are clip-based methods, which means that they only explore a certain part of the holistic video.

2.3 LONG-TERM MODELING FRAMEWORKS

Long-term modeling frameworks have been developed for capture more complex temporal structure for video-level represenation learning. Back to the past, video compositional models were proposed to jointly model local video events in (Laptev et al., 2008), where the temporal pyramid matching was combined with the bag-of-visual-words framework to capture long-term temporal structure. However, the rigid composition only works under some conditions, e.g. prefixed duration and anchor points in time. A mainstream method operated on a continuous video frame sequence with recurrent neural networks Ng et al. (2015); Donahue et al. (2015) with 2D CNNs for frame-level feature extraction. Temporal Segment Network (TSN) (Wang et al., 2016) has been proposed to model video-level temporal information with a sparse sampling and aggregation strategy. TSN sparsely sampled frames from the whole video and these frames are modelled by the same CNN backbone. These scores are averaged to generate video-level prediction. Although originally designed for 2D CNNs, TSN can also be applied to 3D CNNs, which is set as one of the baselines in this paper. One obvious drawback of TSN is that due to the simple average aggregation, it can not model finer temporal structure. Temporal Relational Reasoning Network (TRN) (Zhou et al., 2018) models temporal segment relation by encoding individual representation of each segment with relation networks. TRN is able to model video-level temporal order but lacks capacity of capturing finer temporal structures. Our proposed V4D, however, significantly surpass these previous video-level learning methods on both appearance-dominated video recognition benchmark (e.g., Kinetics) and motion-dominated video recognition benchmark (e.g., Something-Something). V4D framework is able to model both short-term and long-term temporal structures with a unique design of 4D residual block.

3 VIDEO-LEVEL 4D COVOLUTIONAL NEURAL NETWORKS

In this section, we introduce novel **V**ideo-level **4D** Convolution Neural Networks, namely V4D, for video action recognition. This is the first attempt to design 4D convolutions for RGB-based video recognition. Previous methods, such as (You & Jiang, 2018; Choy et al., 2019), utilize 4D CNNs to process videos of point cloud so that their input is 4D data. Instead, our V4D processes videos of RGB frames so that our input is 3D data. This basically makes the methods and tasks quite different.

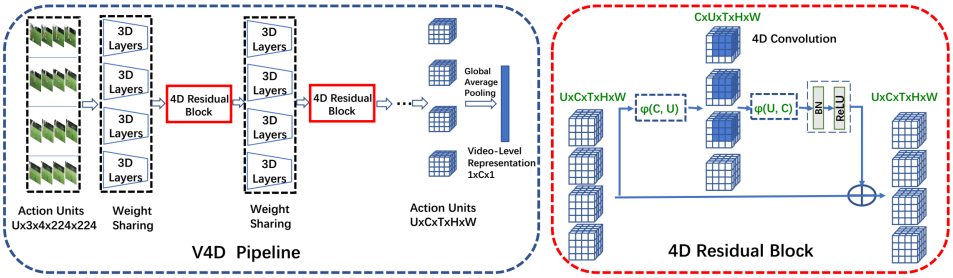

Figure 1: Video-level 4D Convolutional Neural Networks for video recognition.

Existing 3D CNNs take a short-term snippet as input, without considering the evolution of 3D spatio-temporal features for video-level representation. Wang et al. (2018b); Yue et al. (2018); Liu et al. (2019) proposed self-attention mechanisms to model non-local spatio-temporal features, but these methods are originally designed for clip-based 3D CNNs. It remains unclear how to incorporate such operations on holistic video representation, and whether such operations are useful for video-level learning. Our goal is to model 3D spatio-temporal features globally, which can be implemented in a higher dimension. In this work, we introduce new Residual 4D Blocks, which allow us to cast 3D CNNs into 4D CNNs for learning long-range interactions of the 3D features, resulting in a "time of time" video-level representation.

3.1 A VIDEO-LEVEL SAMPLING STRATEGY

To model meaningful video-level representation for action recognition, the input to the networks has to cover the holistic duration of a given video, and at the same time preserve short-term action details. A straightforward approach is to implement per-frame training of the networks yet this is not practical by considering the limit of computation resource. In this work, we uniformly divide the whole video into U sections, and select a snippet from each section to represent a short-term action pattern, called "action unit". Then we have U action units to represent the holistic action in a video. Formally, we denote the video-level input $V = \{A_1, A_2, ..., A_U\}$, where $A_i \in \mathbb{R}^{C\times T\times H\times W}$. During training, each action unit A_i is randomly selected from each U section. During testing, the center of each A_i locates exactly at the center of each section.

3.2 4D CONVOLUTIONS FOR LEARNING SPATIO-TEMPORAL INTERACTIONS

3D Convolutional kernels have been proposed for years, and are powerful to model short-term spatio-temporal features. However, the receptive fields of 3D kernels are often limited due to the small sizes of kernels, and pooling operations are often applied to enlarge the receptive fields, resulting in a significant cost of information loss. This inspired us to develop new operations which are able to model both short- and long-term spatio-temporal representations simultaneously, with easy implementations and fast training. From this prospective, we propose 4D convolutions for better modeling long-range spatio-temporal interactions.

Formally, we denote the input to 4D convolutions as a tensor V of size (C, U, T, H, W), where C is number of channel, U is the number of action units (the fourth dimension in this paper), T, H, W are temporal length, height and width of the action units, respectively. We omit the batch dimension for simplicity. Following the annotations from Ji et al. (2010), a pixel at position (u, t, h, w) of the jth channel in the output is denoted as o_j^{uthw}, a 4D convolution operation can be formulated as :

$$o_j^{uthw} = b_j + \sum_{c}^{C_{in}} \sum_{s=0}^{S-1} \sum_{p=0}^{P-1} \sum_{q=0}^{Q-1} \sum_{r=0}^{R-1} \mathcal{W}_{jc}^{spqr} v_c^{(u+s)(t+p)(h+q)(w+r)} \tag{1}$$

where b_j is the bias term, c is one of the C_{in} input channels of the feature maps from input V, $S \times P \times Q \times R$ is the shape of 4D convolutional kernel, $\mathcal{W}_{jc}^{spqr}$ is the weight at the position (s, p, q, r) of the kernel, corresponding to the c-th channel of the input feature maps and j-th channel of the output feature maps.

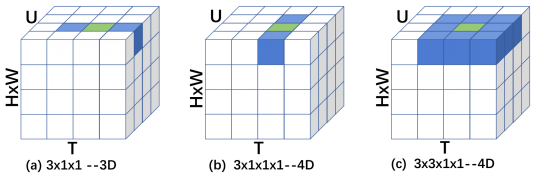

Figure 2: We visualize the implementation of 4D kernels which is compared to that of 3D kernels. U denotes the number of action units, each of which has a shape of T, H, W. Channel and batch dimensions are omitted for clarity. The kernels are colored in Blue, with the center of each kernel colored in Green.

Convolution operation are linear, and the sequence of sum operations in E.q. 1 are exchangeable. Thus we can generate E.q. 2, where the expression in the parentheses can be implemented by 3D convolutions. This is how we implement 4D convolutions with 3D convolutions while most deep learning libraries do not provide 4D convolutional operations.

$$o_j^{uthw} = b_j + \sum_{s=0}^{S-1} (\sum_{c}^{C_{in}} \sum_{p=0}^{P-1} \sum_{q=0}^{Q-1} \sum_{r=0}^{R-1} \mathcal{W}_{jc}^{spqr} v_c^{(u+s)(t+p)(h+q)(w+r)}) \tag{2}$$

With the 4D convolutional kernel, the short-term 3D features of an individual action unit and long-term temporal evolution of multiple action units can be modeled simultaneously in the 4D space. Compared to 3D convolutions, the proposed 4D convolutions are able to model videos in a more meaningful 4D feature space that enables it to learn more complicated interactions of long-range 3D spatio-temporal representations. However, 4D convolutions inevitably introduce more parameters and computation cost. In practice, for example, a 4D convolutional kernel of $k \times k \times k \times k$ employs k times more parameters than a 3D kernel of $k \times k \times k$. Besides $k \times k \times k \times k$ kernels, we also explore $k \times k \times 1 \times 1$ and $k \times 1 \times 1 \times 1$ kernels, for reducing parameters and avoiding the risk of overfitting. The implementations of different kernels are shown in Figure 2.

3.3 Video-level 4D CNN Architecture

In this section, we aim to incorporate 4D convolutions into existing CNN architecture for action recognition. To fully utilize current state-of-the-art 3D CNNs, we propose a new Residual 4D Convolution Block, by designing a 4D convolution in a residual structure (He et al., 2016). This allows it to aggregate both short-term 3D features and long-term evolution of the spatio-temporal representations for video-level action recognition. Specifically, we define a permutation function $\varphi_{(d_i,d_j)} : M^{d_1 \times \ldots \times d_i \times \ldots \times d_j \times \ldots \times d_n} \mapsto M^{d_1 \times \ldots \times d_j \times \ldots \times d_i \times \ldots \times d_n}$, which permutes dimension d_i and d_j of a tensor $M \in \mathbb{R}^{d_1 \times \ldots \times d_n}$. The Residual 4D Convolution Block can be formulated as:

$$\mathcal{Y}_{3D} = \mathcal{X}_{3D} + \varphi_{(U,C)}(\mathcal{F}_{4D}(\varphi_{(C,U)}(\mathcal{X}_{3D}); \mathcal{W}_{4D})) \tag{3}$$

where $\mathcal{F}_{4D}(\mathcal{X}; \mathcal{W}_{4D})$ is the 4D convolution introduced. $\mathcal{X}_{3D}, \mathcal{Y}_{3D} \in \mathbb{R}^{U \times C \times T \times H \times W}$, and U is merged into batch dimension so that $\mathcal{X}_{3D}, \mathcal{Y}_{3D}$ can be directly processed by standard 3D CNNs. Note that we employ φ to permute the dimensions of $\mathcal{X}_{3D}$ from $U \times C \times T \times H \times W$ to $C \times U \times T \times H \times W$ so that it can be processed by 4D convolutions. Then the output of 4D convolution is permuted back to 3D form so that the output dimensions are consistent with $\mathcal{X}_{3D}$. Batch Normalization (Ioffe & Szegedy, 2015) and ReLU activation (Nair & Hinton, 2010) are then applied. The detailed structure is shown in Figure 1.

Theoretically, any 3D CNN structure can be cast to 4D CNNs by integrating our 4D Convolutional Blocks. As shown in previous works (Zolfaghari et al., 2018; Xie et al., 2018; Wang et al., 2018b; Feichtenhofer et al., 2018), better performance can be obtained by applying 2D convolutions at lower layers and 3D convolutions at higher layers of the 3D networks. In our framework, we utilize the "Slowpath" from Feichtenhofer et al. (2018) as our backbone, denoted as I3D-S. Although the original "Slowpath" is designed for ResNet50, we can extend it to I3D-S ResNet18 for further experiments. The detailed structures of our 3D backbones are shown in Table 1.

layer	I3D-S ResNet18	I3D-S ResNet50	output size
conv_1	1×7×7, 64, stride 1, 2, 2	1×7×7, 64, stride 1, 2, 2	4×112×112
res_2	[1×3×3, 64 1×3×3, 64] ×2	[1×1×1, 64 1×3×3, 64 1×1×1, 256] ×3	4×56×56
res_3	[1×3×3, 128 1×3×3, 128] ×2	[1×1×1, 128 1×3×3, 128 1×1×1, 512] ×4	4×28×28
res_4	[3×3×3, 256 3×3×3, 256] ×2	[3×1×1, 256 1×3×3, 256 1×1×1, 1024] ×6	4×14×14
res_5	[3×3×3, 512 3×3×3, 512] ×2	[3×1×1, 512 1×3×3, 512 1×1×1, 2048] ×3	4×7×7
global average pool, fc			1×1×1

Table 1: We use I3D-Slowpath from (Feichtenhofer et al., 2018) as our backbone. The output size of an example is shown in the right column, where the input has a size of 4×224×224. No temporal degenerating is performed in this structure.

3.4 Training and Inference

Training. As shown in Figure 1, the convolutional part of the network is composed of 3D convolution layers and the proposed Residual 4D Blocks. Each action unit is trained individually and in parallel in the 3D convolution layers, which share the same parameters. These individual 3D features computed from each action units are then fed to the Residual 4D Block for modelling the long-term temporal evolution of the consecutive action units. Finally, global average pooling is applied on the sequence of all action units to form a video-level representation.

Inference. Given U action units $\{A_1, A_2, ..., A_U\}$ of a video, we denote U_{train} as the number of action units for training and U_{infer} as the number of action units for inference. U_{train} and U_{infer} are usually different because computation resource is limited in training, but high accuracy is encouraged in inference. We develop a new video-level inference method, which is shown in Algorithm 1. The 3D convolutional layers are denote as N_{3D}, followed by the proposed 4D Blocks, N_{4D}.

Algorithm 1: V4D Inference.

Network : The network structure is divided into two sub-networks by the first 4D Block, namely N_{3D} and N_{4D}.
Input : U_{infer} action units from a holistic video: $\{A_1, A_2, ..., A_{U_{infer}}\}$.
Output : The video-level prediction.

V4D Inference :

1. $\{A_1, A_2, ..., A_{U_{infer}}\}$ are fed into N_{3D}, generating intermediate feature maps for each unit $\{F_1, F_2, ..., F_{U_{infer}}\}$,$F_i \in \mathbb{R}^{C\times T\times H\times W}$;
2. For the U_{infer} intermediate features, we equally divide them into U_{train} sections. Then we select one unit from each section F_{sec_i} and combine these U_{train} units into a video-level intermediate representation $F^{video} = (F_{sec_1}, F_{sec_2}, ..., F_{sec_{U_{train}}})$. These video-level representations form a new set $\{F_1^{video}, F_2^{video}, ..., F_{U_{combined}}^{video}\}$, where $U_{combined} = (U_{infer}/U_{train})^{U_{train}}$, $F_i^{video} \in \mathbb{R}^{U_{train}\times C\times T\times H\times W}$;
3. Each F_i^{video} in set $\{F_1^{video}, F_2^{video}, ..., F_{U_{combined}}^{video}\}$ are processed by N_{4D} to form a prediction score set $\{P_1, P_2, ..., P_{U_{combined}}\}$;
4. $\{P_1, P_2, ..., P_{U_{combined}}\}$ are averaged to give the final video-level prediction.

3.5 Discussion

In this section, we will show that the proposed V4D can be considered as a 4D generalization of a number of recent widely-applied methods, which may partially explain why V4D works practically well on learning meaningful video-level representation.

Temporal Segment Network. Our V4D is closely related to Temporal Segment Network (TSN). Although originally designed for 2D CNN, TSN can be directly applied to 3D CNN to model video-

level representation. It also employs a video-level sampling strategy with each action unit named "segment". During training, each segment is calculated individually and the prediction scores after the fully-connected layer are then averaged. Since the fully-connected layer is a linear classifier, it is mathematically identical to calculating the average before the fully-connected layer (similar to our global average pooling) or after the fully-connected layer (similar to TSN). Thus our V4D can be considered as 3D CNN + TSN if all parameters in 4D Blocks are assigned zero.

Dilated Temporal Convolution. One special form of 4D convolution kernel, $k \times 1 \times 1 \times 1$, is closely related to Temporal Dilated Convolution (Lea et al., 2016). The input tensor V can be considered as a $(C, U \times T, H, W)$ tensor when all action units are concatenated along the temporal dimension. In this case, the $k \times 1 \times 1 \times 1$ 4D convolution can be considered as a dilated 3D convolution kernel of $k \times 1 \times 1$ with a dilation of T frames. Note that the $k \times 1 \times 1 \times 1$ kernel is just the simplest form of our 4D convolutions, while our V4D architectures utilize more complex kernels and thus can be more meaningful for learning stronger video representation. Furthermore, our 4D Blocks utilize residual connections, ensuring that both long-term and short-term representation can be learned jointly. Simply applying the dilated convolution might discard the short-term fine-grained features.

4 EXPERIMENTS

4.1 DATASETS

We conduct experiments on three standard benchmarks: Mini-Kinetics (Xie et al., 2018), Kinetics-400 (Carreira & Zisserman, 2017), and Something-Something-v1 (Goyal et al., 2017). Mini-kinetics dataset covers 200 action classes, and is a subset of Kinetics-400. Since some videos are no longer available for Kinetics dataset, our version of Kinetics-400 contains 240,436 and 19,796 videos in the training and validation subsets, respectively. Our version of Mini-kinetics contains 78,422 videos for training, and 4,994 videos for validation. Each video has around 300 frames. Something-Something-v1 contains 108,499 videos totally, with 86,017 for training, 11,522 for validation, and 10,960 for testing. Each video has 36 to 72 frames.

4.2 ABLATION STUDY ON MINI-KINETICS

We use pre-trained weights from ImageNet to initialize the model. For training, we adapt the holistic sampling strategy mentioned in section 3.1. We uniformly divide the whole video into U sections, and randomly select a clip of 32 frames from each section. For each clip, by following the sampling strategy in Feichtenhofer et al. (2018), we uniformly sample 4 frames with a fixed stride of 8 to form an action unit. We will study the impact of U in the following experiments. We first resize every frame to 320×256, and then randomly cropping is applied as Wang et al. (2018b). Then the cropped region is further resized to 224×224. We utilize SGD optimizer with an initial learning rate of 0.01, weight decay is set to 10^{-5} with a momentum of 0.9. The learning rate drops by 10 at epoch 35, 60, 80 and the model is trained for 100 epochs in total.

To make a fair comparison, we use spatial fully convolutional testing by following Wang et al. (2018b); Yue et al. (2018); Feichtenhofer et al. (2018). We sample 10 action units evenly from a full-length video, and crop 256×256 regions to spatially cover the whole frame for each action unit. Then we apply the proposed V4D inference. Note that, for the original TSN, 25 clips and 10-crop testing are used during inference. To make a fair comparison between I3D and our V4D, we instead apply this 10 clips and 3-crop inference strategy for TSN.

Results and Effectiveness. To verify the effectiveness of V4D, we compare it with the clip-based method I3D-S, and video-based method TSN+3D CNN. To compensate the extra parameters introduced by 4D blocks, we add a $3 \times 3 \times 3$ residual block at res4 for I3D-S for a fair comparison, denoted as I3D-S ResNet18++. As shown in Table 2a, even V4D uses 4 times less frames than I3D-S during inference and with less parameters than I3D-S ResNet18++, V4D still obtain a 2.0% higher top-1 accuracy than I3D-S. Comparing with current state-of-the-art video-level method TSN+3D CNN, V4D significantly outperforms it by 2.6% top-1 accuracy, by using the same protocol for training and inference.

Different Forms of 4D Convolution Kernels. As mentioned, our 4D convolution kernels can use 3 typical forms: $k \times 1 \times 1 \times 1$, $k \times k \times 1 \times 1$ and $k \times k \times k \times k$. In this experiment, we set $k = 3$ for

model	T_{train} $\times U_{train}$	T_{infer} $\times U_{infer}$ $\times$ #crop	top-1	top5	parameters
I3D-S ResNet18	4×1	$4 \times 10 \times 3$	72.2	91.2	32.3M
I3D-S ResNet18	16×1	$16 \times 10 \times 3$	73.4	91.1	32.3M
I3D-S ResNet18++	16×1	$16 \times 10 \times 3$	73.6	91.5	34.1M
TSN+I3D-S ResNet18	4×4	$4 \times 10 \times 3$	73.0	91.3	32.3M
V4D ResNet18	4×4	$4 \times 10 \times 3$	75.6	92.7	33.1M

(a) Effectiveness of V4D. T represents temporal length of each action unit. U represents the number of action units.

model	input size	flops
I3D-S ResNet18	$16 \times 256 \times 256$	55.1G
TSN+I3D-S ResNet18	$4 \times 4 \times 256 \times 256$	55.1G
V4D ResNet18	$4 \times 4 \times 256 \times 256$	58.8G

(b) Forward flops of previous works and V4D. One 4D block at res3 and one at res4 for V4D.

model	form of 4D kernel	top-1	top5
I3D-S ResNet18	-	72.2	91.2
TSN+I3D-S ResNet18	-	73.0	91.3
V4D ResNet18	$3 \times 1 \times 1 \times 1$	73.8	92.0
V4D ResNet18	$3 \times 3 \times 1 \times 1$	74.5	92.4
V4D ResNet18	$3 \times 3 \times 3 \times 3$	74.7	92.5

(c) Different Forms of 4D Convolution Kernel.

model	4D kernel	top-1	top5
I3D-S ResNet18	-	72.2	91.2
TSN+I3D-S ResNet18	-	73.0	91.3
V4D ResNet18	1 at res3	74.2	92.3
V4D ResNet18	1 at res4	74.5	92.4
V4D ResNet18	1 at res5	73.6	91.4
V4D ResNet18	1 at res3, 1 at res4	75.6	92.7

(d) Position and Number of 4D Blocks.

model	U_{train}	top-1	top5
I3D-S ResNet18	1	72.2	91.2
TSN+I3D-S ResNet18	4	73.0	91.3
V4D ResNet18	3	74.3	92.2
V4D ResNet18	4	74.5	92.4
V4D ResNet18	5	74.5	92.3
V4D ResNet18	6	74.6	92.5

(e) Effect of U_{train}.

Table 2: **Ablations** on Mini-Kinetics, with top-1 and top-5 classification accuracy (%).

simplicity, and apply a single 4D block at the end of res4 in I3D-S ResNet18. As shown in Table 2c, V4D with $3 \times 3 \times 3 \times 3$ kernel can achieve the highest performance. However, by considering the trade-off between model parameters and performance, we use the $3 \times 3 \times 1 \times 1$ kernel in the following experiments.

Position and Number of 4D Blocks. We evaluate the impact of position and number of 4D Blocks for our V4D. We investigate the performance of V4D by using one $3 \times 3 \times 1 \times 1$ 4D block at res3, res4 or res5. As shown in Table 2d, a higher accuracy can be obtained by applying the 4D block at res3 or res4, indicating that the merged long-short term features of the 4D block need to be further refined by 3D convolutions to generate more meaningful representation. Furthermore, inserting one 4D block at res3 and one at res4 can achieve a higher accuracy.

Number of Action Units U. We further evaluate our V4D by using different numbers of action units for training, with different values of hyperparameter U. In this experiment, one $3 \times 3 \times 1 \times 1$ Residual 4D block is inserted at the end of res4 of ResNet18. As shown in Table 2e, U does not have a significant impact on the performance, which suggests that: (1) V4D is a video-level feature learning model, which is robust against the number of short-term units; (2) an action generally does not contain many stages, and thus increasing U is not helpful. Also, the number of action units increasing means that the fourth dimension is increasing, which needs a larger 4D kernel to cover the long-range evolution of spatio-temporal representation.

Comparison with State-Of-The-Art. We compare our V4D with previous state-of-the-art methods on Mini-Kinetics. 4D Residual Blocks are added into every other 3D residual blocks in res3 and res4. With much fewer frames utilized during training and inference, our V4D ResNet50 achieves a higher accuracy than all reported results on this benchmark, which is even higher than 3D ResNet101 with 5 Compact Generalized Non-local Blocks. Note that our V4D ResNet18 can achieve a higher accuracy than 3D ResNet50, which further verify the effectiveness of our V4D structure.

4.3 Results on Kinetics

We further conduct experiments on large-scale video recognition benchmark, Kinetics-400, to evaluate the capability of our V4D. To make a fair comparison, we utilize ResNet50 as backbone for V4D. The training and inference sampling strategy is identical to previous section, except that each action unit now contains 8 frames instead of 4. We set $U = 4$ so that there are 8×4 frames in total for training. Due to the limit of computation resource, we choose to train the model in multiple stages. We first train the 3D ResNet50 backbone with 8-frame inputs. Then we load the 3D ResNet50 weights to

Model	Backbone	$T_{train} \times U_{train}$	$T_{infer} \times U_{infer} \times$ #crop	top-1	top5
S3D (Xie et al., 2018)	S3D Inception	64×1	N/A	78.9	-
I3D (Yue et al., 2018)	3D ResNet50	32×1	$32 \times 10 \times 3$	75.5	92.2
I3D (Yue et al., 2018)	3D ResNet101	32×1	$32 \times 10 \times 3$	77.4	93.2
I3D+NL (Yue et al., 2018)	3D ResNet50	32×1	$32 \times 10 \times 3$	77.5	94.0
I3D+CGNL (Yue et al., 2018)	3D ResNet50	32×1	$32 \times 10 \times 3$	78.8	94.4
I3D+NL (Yue et al., 2018)	3D ResNet101	32×1	$32 \times 10 \times 3$	79.2	93.2
I3D+CGNL (Yue et al., 2018)	3D ResNet101	32×1	$32 \times 10 \times 3$	79.9	93.4
V4D(Ours)	V4D ResNet18	4×4	$4 \times 10 \times 3$	75.6	92.7
V4D(Ours)	V4D ResNet50	4×4	$4 \times 10 \times 3$	80.7	95.3

Table 3: Comparison with state-of-the-art on Mini-Kinetics. T indicates temporal length of each action unit. U represents the number of action units.

V4D ResNet50, with all 4D Blocks fixed to zero. The V4D ResNet50 is then fine-tuned with 8×4 input frames. Finally, we optimize all 4D Blocks and train the V4D with 8×4 frames.

As shown in Table 4, our V4D achieves competitive results on Kinetics-400 benchmark.

Model	Backbone	top-1	top-5
ARTNet with TSN (Wang et al., 2018a)	ARTNet ResNet18	70.7	89.3
ECO (Zolfaghari et al., 2018)	BN-Inception+3D ResNet18	70.0	89.4
S3D-G (Xie et al., 2018)	S3D Inception	74.7	93.4
Nonlocal Network (Wang et al., 2018a)	3D ResNet50	76.5	92.6
SlowFast (Feichtenhofer et al., 2018)	SlowFast ResNet50	77.0	92.6
I3D(Carreira & Zisserman, 2017)	I3D Inception	72.1	90.3
Two-stream I3D(Carreira & Zisserman, 2017)	I3D Inception	75.7	92.0
I3D-S(Feichtenhofer et al., 2018)	Slow pathway ResNet50	74.9	91.5
V4D(Ours)	V4D ResNet50	77.4	93.1

Table 4: Comparison with state-of-the-art on Kinetics.

4.4 Results on Something-Something-v1

Something-Something is a rather different dataset compared to Mini-Kinetics and Kinetics. Instead of enhancing high-level action concepts, Something-Something focuses on modeling temporal information and motion. The background is much cleaner than Kinetics but the motions of action categories are much more complicated. Each video in Something-Something contains one single and continuous action with clear start and end on temporal dimension.

Comparison with Prior Works. As shown in Table 4.4, our V4D achieves competitive results on the Something-Something-v1. We use V4D ResNet50 pre-trained on Kinetics for experiments.

Model	Backbone	top-1
MultiScale TRN (Zhou et al., 2018)	BN-Inception	34.4
ECO (Zolfaghari et al., 2018)	BN-Inception+3D ResNet18	46.4
S3D-G (Xie et al., 2018)	S3D Inception	45.8
Nonlocal Network+GCN (Wang & Gupta, 2018)	3D ResNet50	46.1
TrajectoryNet (Zhao et al., 2018)	S3D ResNet18	47.8
V4D(Ours)	V4D ResNet50	50.4

Table 5: Comparison with state-of-the-art on Something-Something-v1.

Temporal Order As shown in Xie et al. (2018), the performance can drop considerably by reversing the temporal order of short-term 3D features, which demonstrates that the strong temporal order information has been learned by 3D CNNs. For our V4D, there are two levels of temporal order, a short-term order and a long-term order. As shown in Table 6, either by reversing the frames inside each action unit or by reversing the sequence of action units, the top-1 accuracy drops significantly, which indicates that our V4D is able to capture both long-term and short-term temporal order.

Action Unit Temporal Order	Video-level Temporal Order	top-1
Normal	Normal	50.4
Normal	Reversed	20.1
Reversed	Normal	17.2

Table 6: V4D is able to capture the arrow of time.

5 CONCLUSIONS

We have introduced new Video-level 4D Convolutional Neural Networks, namely V4D, to learn strong temporal evolution of long-range spatio-temporal representation, as well as retaining 3D features with residual connections. In addition, we further introduce the training and inference methods for our V4D. Experiments were conducted on three video recognition benchmarks, where our V4D achieved the state-of-the-art results.

REFERENCES

João Carreira and Andrew Zisserman. Quo vadis, action recognition? A new model and the kinetics dataset. In *CVPR*, pp. 4724–4733. IEEE Computer Society, 2017.

Christopher Bongsoo Choy, JunYoung Gwak, and Silvio Savarese. 4d spatio-temporal convnets: Minkowski convolutional neural networks. *CoRR*, abs/1904.08755, 2019.

Jeffrey Donahue, Lisa Anne Hendricks, Sergio Guadarrama, Marcus Rohrbach, Subhashini Venugopalan, Kate Saenko, and Trevor Darrell. Long-term recurrent convolutional networks for visual recognition and description. In *CVPR*, pp. 2625–2634, 2015.

Alexey Dosovitskiy, Philipp Fischer, Eddy Ilg, Philip Häusser, Caner Hazirbas, Vladimir Golkov, Patrick van der Smagt, Daniel Cremers, and Thomas Brox. Flownet: Learning optical flow with convolutional networks. In *ICCV*, pp. 2758–2766. IEEE Computer Society, 2015.

Christoph Feichtenhofer, Haoqi Fan, Jitendra Malik, and Kaiming He. Slowfast networks for video recognition. *CoRR*, abs/1812.03982, 2018.

Raghav Goyal, Samira Ebrahimi Kahou, Vincent Michalski, Joanna Materzynska, Susanne Westphal, Heuna Kim, Valentin Haenel, Ingo Fründ, Peter Yianilos, Moritz Mueller-Freitag, Florian Hoppe, Christian Thurau, Ingo Bax, and Roland Memisevic. The "something something" video database for learning and evaluating visual common sense. In *ICCV*, pp. 5843–5851. IEEE Computer Society, 2017.

Kaiming He, Xiangyu Zhang, Shaoqing Ren, and Jian Sun. Deep residual learning for image recognition. In *CVPR*, pp. 770–778. IEEE Computer Society, 2016.

Fabian Caba Heilbron, Victor Escorcia, Bernard Ghanem, and Juan Carlos Niebles. Activitynet: A large-scale video benchmark for human activity understanding. In *IEEE Conference on Computer Vision and Pattern Recognition, CVPR 2015, Boston, MA, USA, June 7-12, 2015*, pp. 961–970. IEEE Computer Society, 2015. doi: 10.1109/CVPR.2015.7298698. URL https://doi.org/10.1109/CVPR.2015.7298698.

Sergey Ioffe and Christian Szegedy. Batch normalization: Accelerating deep network training by reducing internal covariate shift. In *ICML*, volume 37 of *JMLR Workshop and Conference Proceedings*, pp. 448–456. JMLR.org, 2015.

Shuiwang Ji, Wei Xu, Ming Yang, and Kai Yu. 3d convolutional neural networks for human action recognition. *IEEE Transactions on Pattern Analysis and Machine Intelligence*, 35:221–231, 2010.

Ivan Laptev, Marcin Marszalek, Cordelia Schmid, and Benjamin Rozenfeld. Learning realistic human actions from movies. In *2008 IEEE Computer Society Conference on Computer Vision and Pattern Recognition (CVPR 2008), 24-26 June 2008, Anchorage, Alaska, USA*. IEEE Computer Society, 2008. doi: 10.1109/CVPR.2008.4587756. URL https://doi.org/10.1109/CVPR.2008.4587756.

Colin Lea, René Vidal, Austin Reiter, and Gregory D. Hager. Temporal convolutional networks: A unified approach to action segmentation. In *ECCV Workshops (3)*, volume 9915 of *Lecture Notes in Computer Science*, pp. 47–54, 2016.

Xingyu Liu, Joon-Young Lee, and Hailin Jin. Learning video representations from correspondence proposals. *CoRR*, abs/1905.07853, 2019.

Vinod Nair and Geoffrey E. Hinton. Rectified linear units improve restricted boltzmann machines. In *ICML*, pp. 807–814. Omnipress, 2010.

Joe Yue-Hei Ng, Matthew Hausknecht, Sudheendra Vijayanarasimhan, Oriol Vinyals, Rajat Monga, and George Toderici. Beyond short snippets: Deep networks for video classification. In *CVPR*, pp. 4694–4702, 2015.

A. J. Piergiovanni and Michael S. Ryoo. Representation flow for action recognition. *CoRR*, abs/1810.01455, 2018.

Zhaofan Qiu, Ting Yao, and Tao Mei. Learning spatio-temporal representation with pseudo-3d residual networks. *2017 IEEE International Conference on Computer Vision (ICCV)*, pp. 5534–5542, 2017.

Karen Simonyan and Andrew Zisserman. Two-stream convolutional networks for action recognition in videos. In *NIPS*, pp. 568–576, 2014.

Shuyang Sun, Zhanghui Kuang, Lu Sheng, Wanli Ouyang, and Wei Zhang. Optical flow guided feature: A fast and robust motion representation for video action recognition. In *CVPR*, pp. 1390–1399. IEEE Computer Society, 2018.

Du Tran, Lubomir D. Bourdev, Rob Fergus, Lorenzo Torresani, and Manohar Paluri. Learning spatiotemporal features with 3d convolutional networks. In *ICCV*, pp. 4489–4497. IEEE Computer Society, 2015.

Limin Wang, Yuanjun Xiong, Zhe Wang, Yu Qiao, Dahua Lin, Xiaoou Tang, and Luc Van Gool. Temporal segment networks: Towards good practices for deep action recognition. In *ECCV (8)*, volume 9912 of *Lecture Notes in Computer Science*, pp. 20–36. Springer, 2016.

Limin Wang, Wei Li, Wen Li, and Luc Van Gool. Appearance-and-relation networks for video classification. In *CVPR*, pp. 1430–1439. IEEE Computer Society, 2018a.

Xiaolong Wang and Abhinav Gupta. Videos as space-time region graphs. In *ECCV (5)*, volume 11209 of *Lecture Notes in Computer Science*, pp. 413–431. Springer, 2018.

Xiaolong Wang, Ross B. Girshick, Abhinav Gupta, and Kaiming He. Non-local neural networks. In *CVPR*, pp. 7794–7803. IEEE Computer Society, 2018b.

Saining Xie, Chen Sun, Jonathan Huang, Zhuowen Tu, and Kevin Murphy. Rethinking spatiotemporal feature learning: Speed-accuracy trade-offs in video classification. In *ECCV (15)*, volume 11219 of *Lecture Notes in Computer Science*, pp. 318–335. Springer, 2018.

Quanzeng You and Hao Jiang. Action4d: Real-time action recognition in the crowd and clutter. *ArXiv*, abs/1806.02424, 2018.

Kaiyu Yue, Ming Sun, Yuchen Yuan, Feng Zhou, Errui Ding, and Fuxin Xu. Compact generalized non-local network. In *NeurIPS*, pp. 6511–6520, 2018.

Bowen Zhang, Limin Wang, Zhe Wang, Yu Qiao, and Hanli Wang. Real-time action recognition with enhanced motion vector CNNs. In *CVPR*, pp. 2718–2726, 2016.

Yue Zhao, Yuanjun Xiong, and Dahua Lin. Trajectory convolution for action recognition. In *NeurIPS*, pp. 2208–2219, 2018.

Bolei Zhou, Aditya Khosla, Àgata Lapedriza, Aude Oliva, and Antonio Torralba. Learning deep features for discriminative localization. In *2016 IEEE Conference on Computer Vision and Pattern Recognition, CVPR 2016, Las Vegas, NV, USA, June 27-30, 2016*, pp. 2921–2929. IEEE Computer Society, 2016. doi: 10.1109/CVPR.2016.319. URL `https://doi.org/10.1109/CVPR.2016.319`.

Bolei Zhou, Alex Andonian, Aude Oliva, and Antonio Torralba. Temporal relational reasoning in videos. In *ECCV (1)*, volume 11205 of *Lecture Notes in Computer Science*, pp. 831–846. Springer, 2018.

Mohammadreza Zolfaghari, Kamaljeet Singh, and Thomas Brox. ECO: efficient convolutional network for online video understanding. In *ECCV (2)*, volume 11206 of *Lecture Notes in Computer Science*, pp. 713–730. Springer, 2018.

A APPENDIX

A.1 EXTENDED EXPERIMENTS ON LARGE-SCALE UNTRIMMED VIDEO RECOGNITION

In order to check the generalization ability of our proposed V4D, we also conduct experiments for untrimmed video classification. To be specific, we choose ActivityNet v1.3 Heilbron et al. (2015), which is a large-scale untrimmed video dataset, containing videos of 5 to 10 minutes and typically large time lapses of the videos are not related with any activity of interest. We adopt V4D ResNet50 to compare with previous works. During inference, Multi-scale Temporal Window Integration is applied following (Wang et al., 2016). The evaluation metric is mean average precision (mAP) for action recognition. Note that only RGB modality is used as input.

Model	Backbone	mAP
TSN Wang et al. (2016)	BN-Inception	79.7
TSN Wang et al. (2016)	Inception V3	83.3
TSN-Top3 Wang et al. (2016)	Inception V3	84.5
V4D(Ours)	V4D ResNet50	88.9

Table 7: Comparison with state-of-the-art on ActivityNet v1.3.

A.2 VISUALIZATION

We implement 3D CAM based on Zhou et al. (2016), which was originally implemented for 2D cases. Generally, class activation maps (CAM) imply which areas are most important for classification. Here we show some random visualization results from validation set of Mini-Kinetics, where TSN + I3D-S ResNet18 generates wrong prediction while V4D ResNet18 generates correct prediction. The original RGB frames are shown in the first row. The second row shows the CAMs of TSN + I3D-S ResNet18. The third row shows the CAMs of V4D ResNet18.

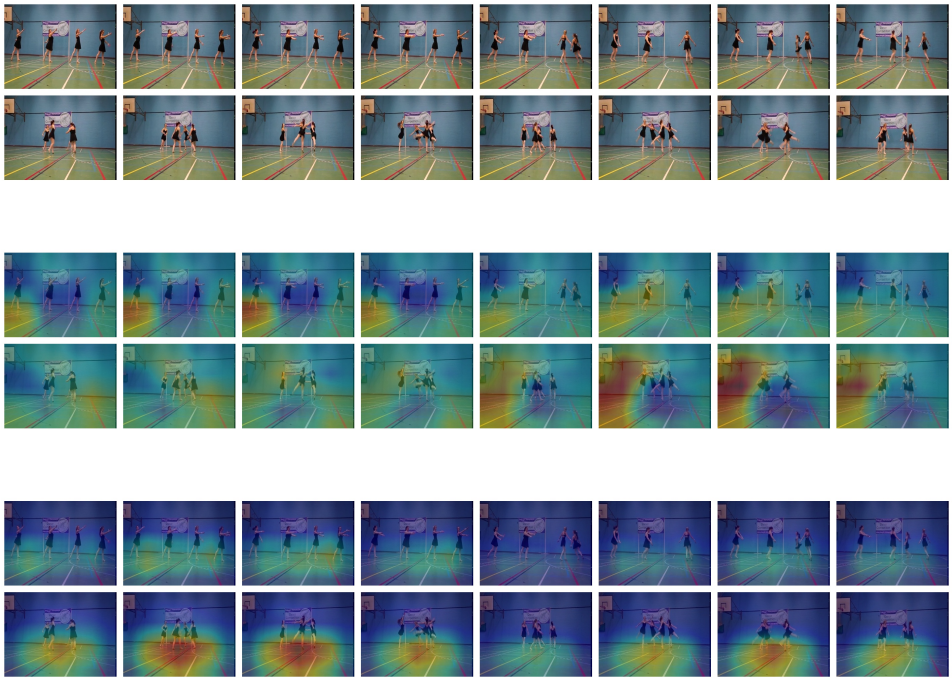

Figure 3:

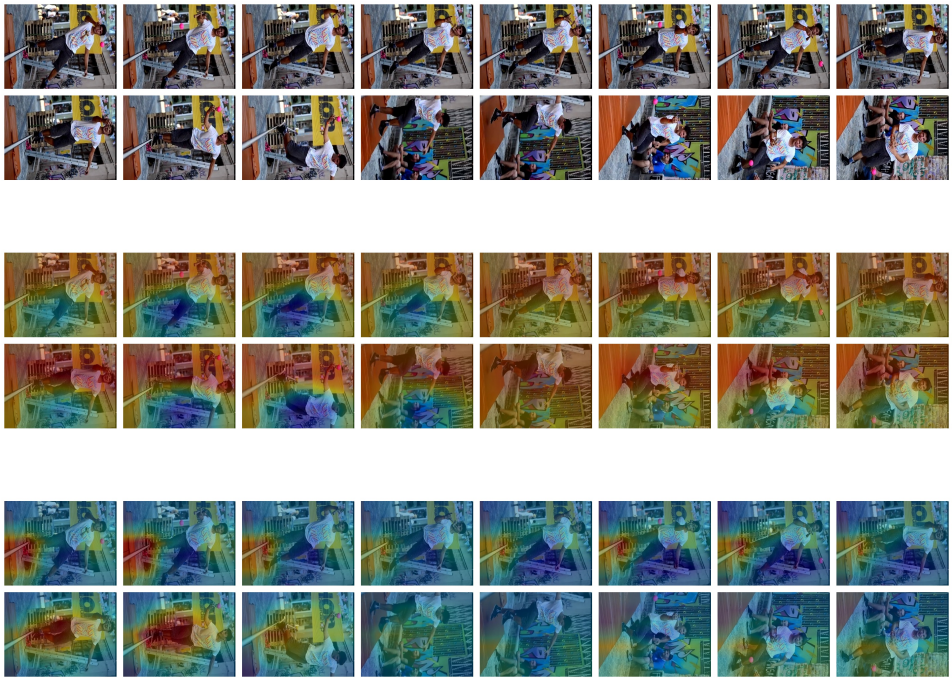

Figure 4:

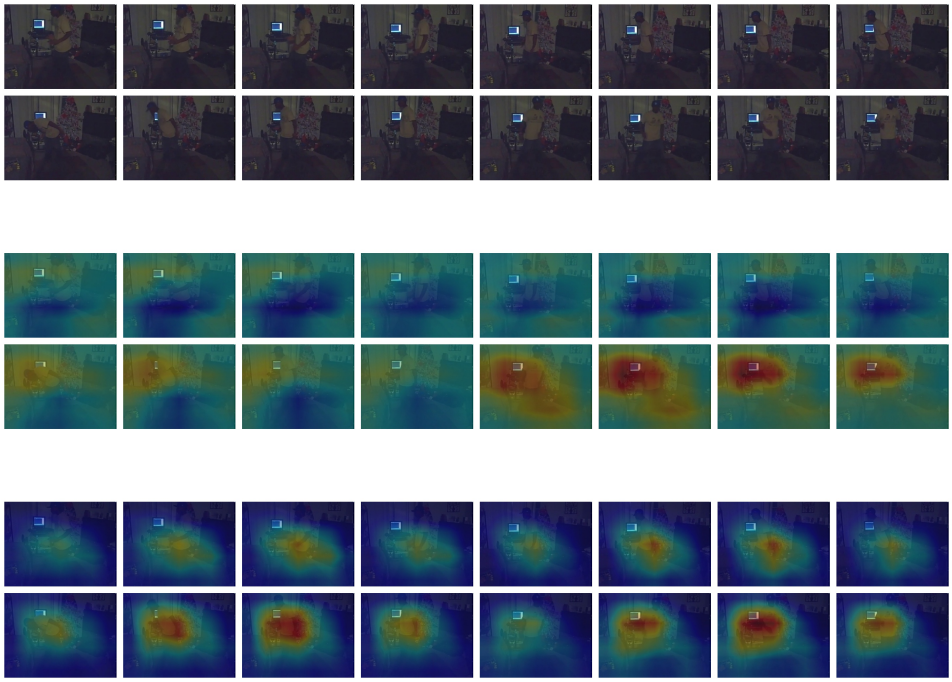

Figure 5:

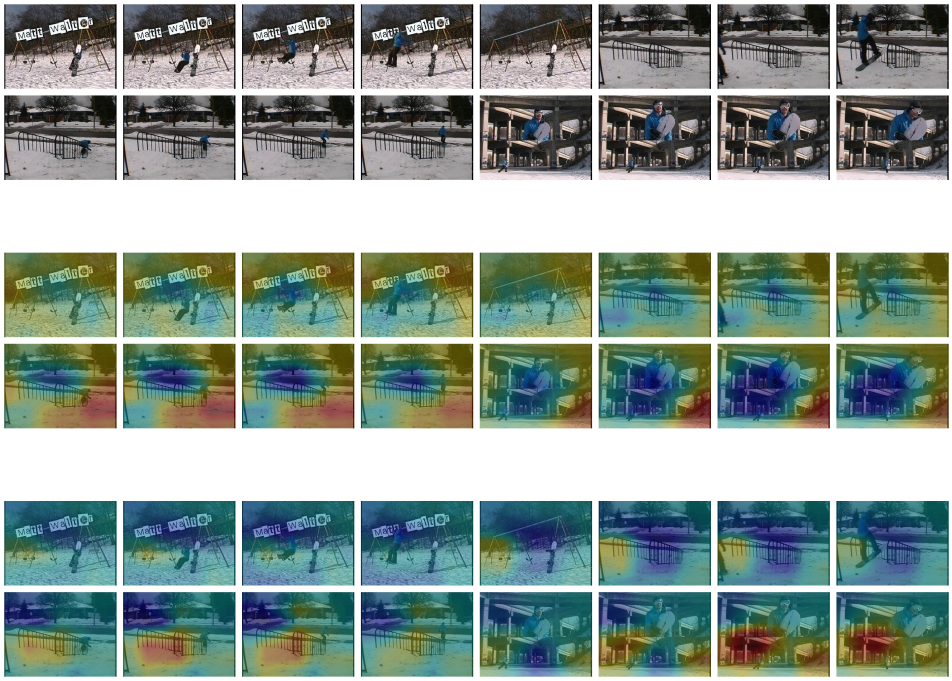

Figure 6:

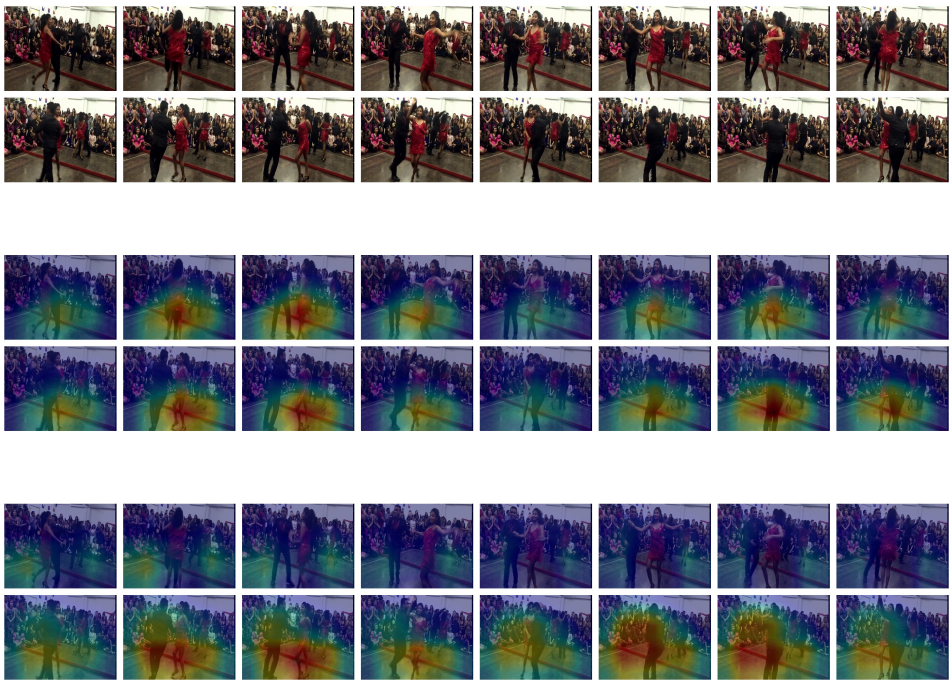

Figure 7:

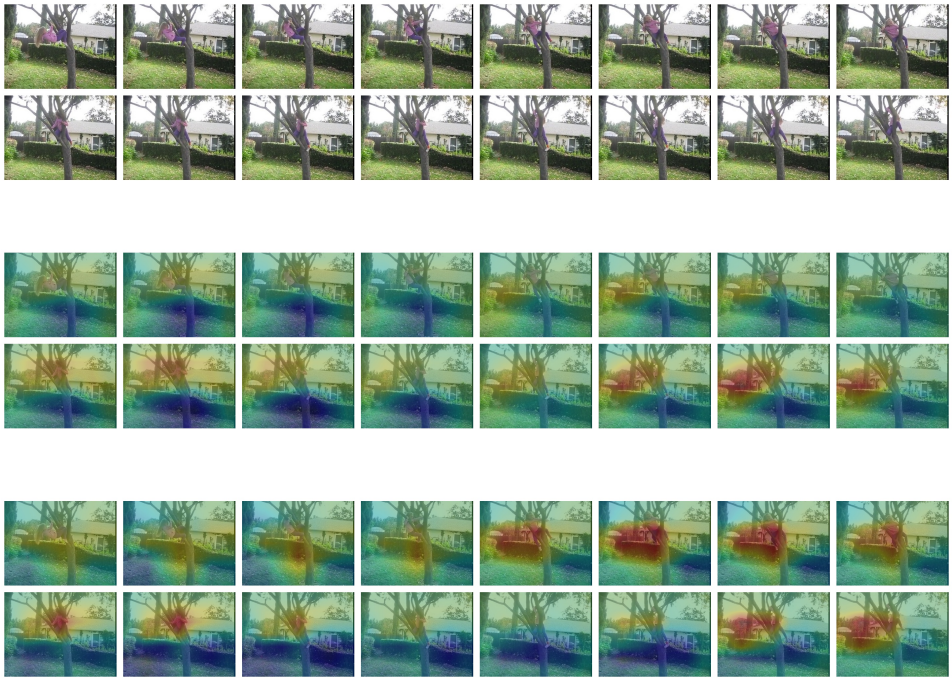

Figure 8:

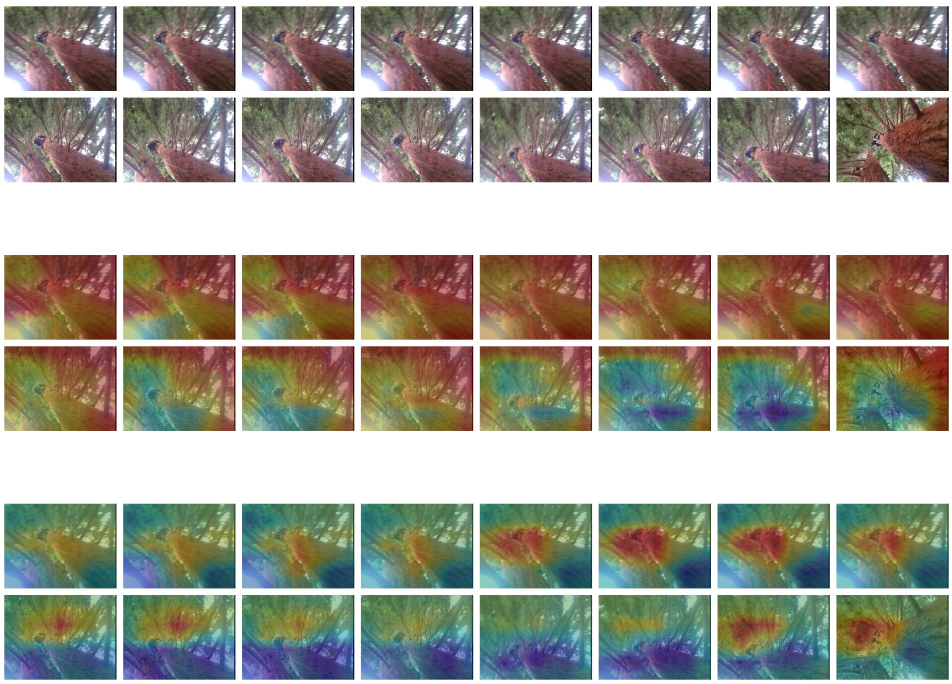

Figure 9:

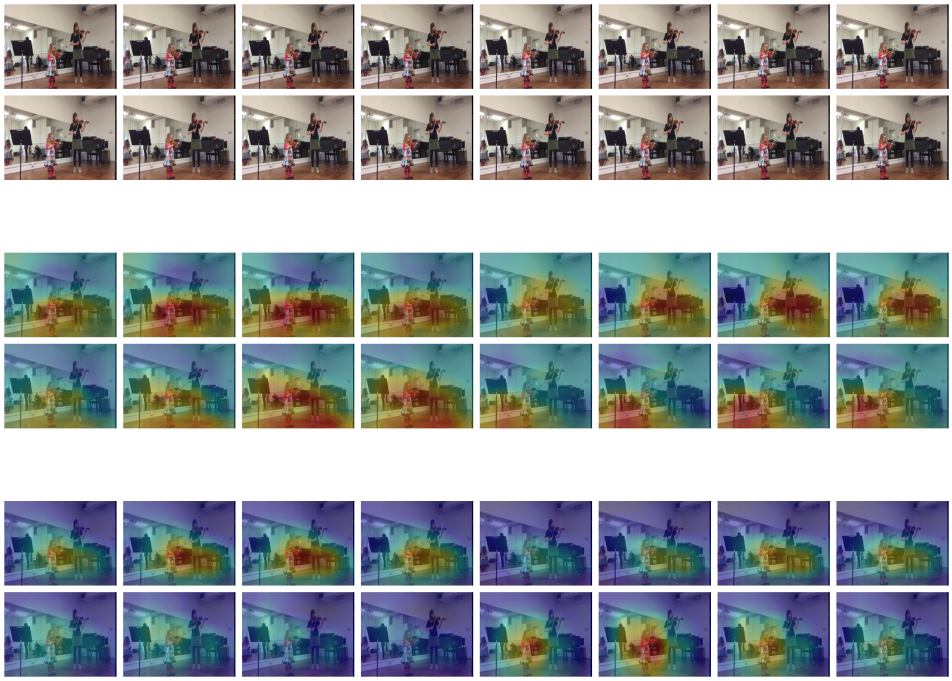

Figure 10:

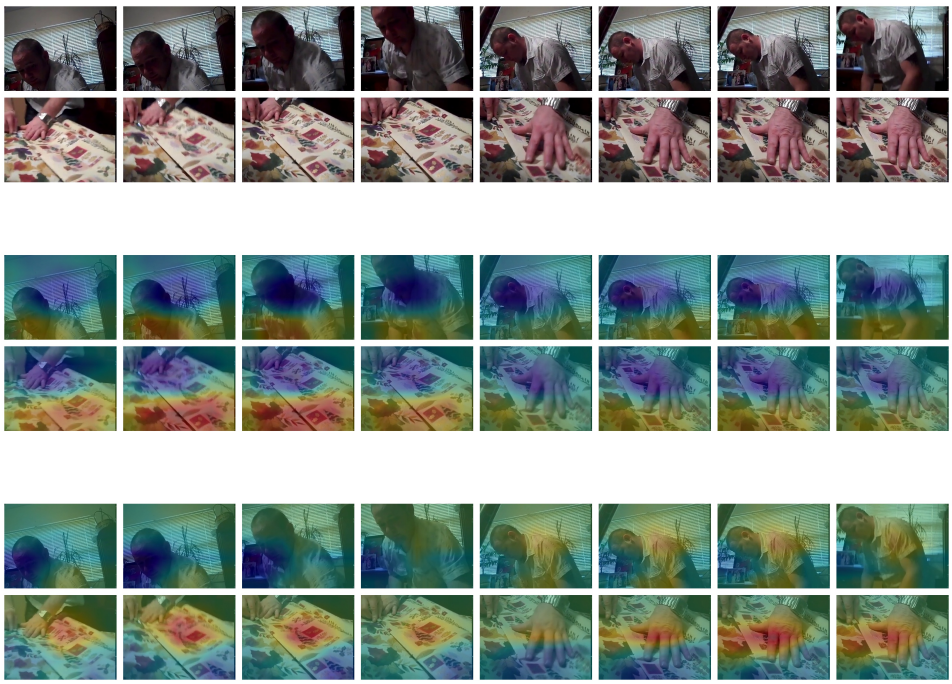

Figure 11:

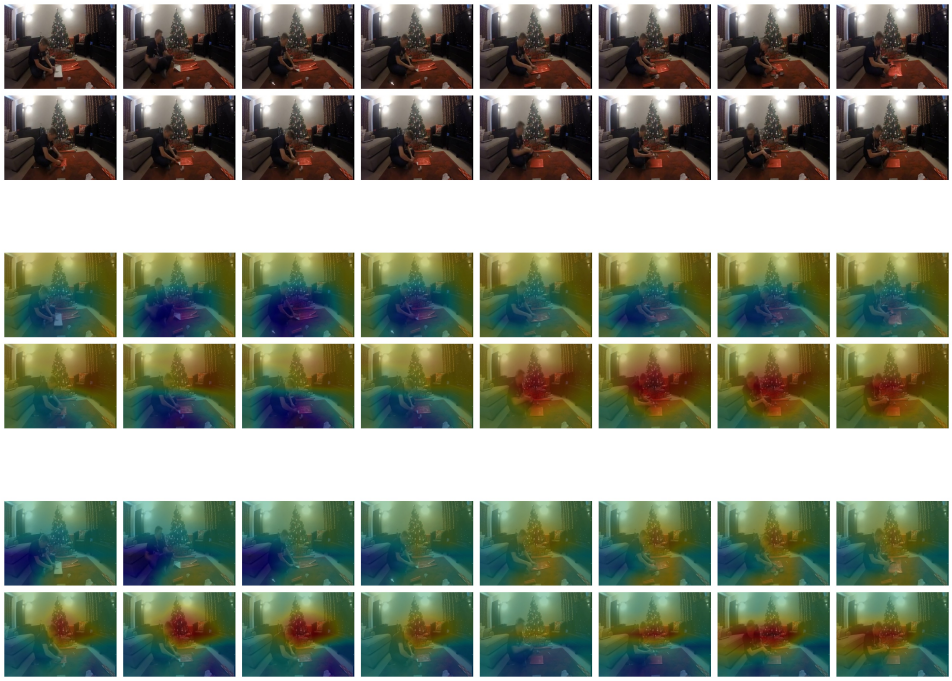

Figure 12:

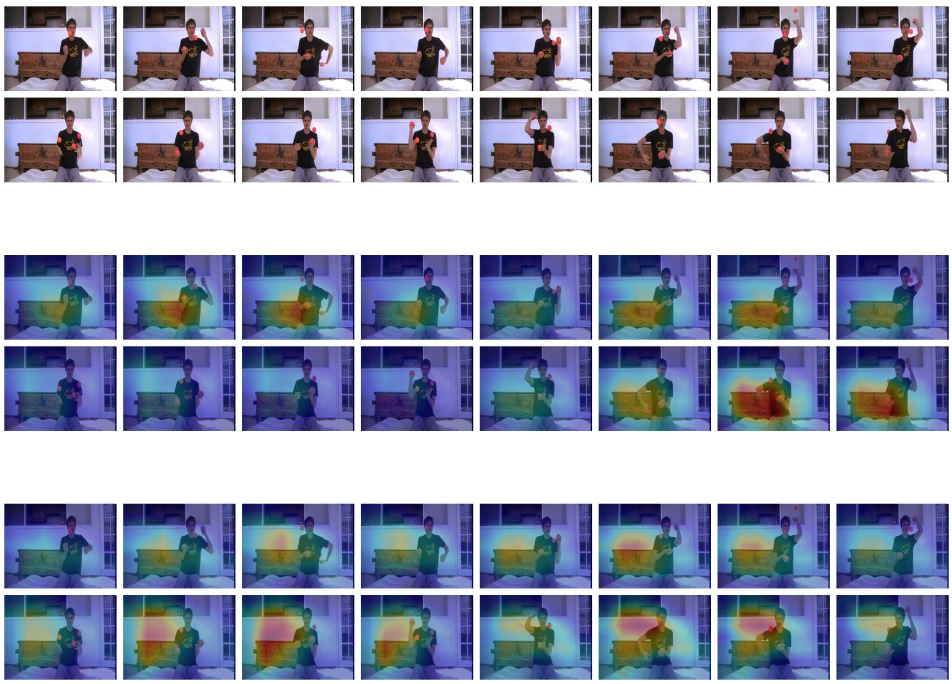

Figure 13: